Status and First Results of the KLOE Detector

The KLOE collaboration [1]
presented by

Achim G. Denig[2]
INFN - Laboratori Nazionali di Frascati

The KLOE detector at the Frascati ϕ factory DAΦNE has the major goal of measuring direct CP violation in the neutral kaon system, while having the opportunity to perform a large variety of other measurements in the field of electroweak and hadronic physics. The experiment has started taking data in 1999 during the commissioning of the machine. The performance of the different detector components, the calibration techniques and some preliminary studies for the CP measurements are presented. A first data sample of $2.4pb^{-1}$ has been used to study the radiative decays of the ϕ and of the decay $\phi \to \pi^+\pi^-\pi^0$. The preliminary results are reported in this paper.

1 Physics at the ϕ factory DAΦNE

DAΦNE is a double annular e^+e^- collider on the ϕ resonance $\sqrt{s} = 1020$ MeV which has been designed for a peak luminsity of $5 \cdot 10^{32} cm^{-2}s^{-1}$ [1]. The $\phi(1020)$ vector meson is predominantly decaying into kaon pairs, where the decay into the neutral pair $K^0\bar{K}^0$ (i.e. $K_S K_L$) is of special interest, since it opens the possibility to study CP

[1] The KLOE collaboration: M. Adinolfi, A. Aloisio, F. Ambrosino, A. Andryakov, A. Antonelli, M. Antonelli, F. Anulli, C. Bacci, G. Barbiellini, F. Bellini, G. Bencivenni, S. Bertolucci, C. Bini, C. Bloise, V. Bocci, F. Bossi, P. Branchini, S. A. Bulychjov, G. Cabibbo, A. Calcaterra, R. Caloi, P. Campana, G. Capon, G. Carboni, A. Cardini, M. Casarsa, V. Casavola, G. Cataldi, F. Ceradini, F. Cervelli, F. Cevenini, G. Chiefari, P. Ciambrone, S. Conetti, E. De Lucia, G. De Robertis, R. De Sangro, P. De Simone, G. De Zorzi, S. Dell'Agnello, A. Denig, A. Di Domenico, C. Di Donato, S. Di Falco, A. Doria, E. Drago, O. Erriquez, A. Farilla, G. Felici, A. Ferrari, M. L. Ferrer, G. Finocchiaro, C. Forti, A. Franceschi, P. Franzini, M. L. Gao, C. Gatti, P. Gauzzi, S. Giovannella, V. Golovatyuk, E. Gorini, F. Grancagnolo, W. Grandegger, E. Graziani, P. Guarnaccia, H. G. Han, S. W. Han, X. Huang, M. Incagli, L. Ingrosso, Y. Y. Jiang, W. Kim, W. Kluge, C. Kuo, V. Kulikov, F. Lacava, G. Lanfranchi, J. Lee-Franzini, T. Lomtadze, C. Luisi, C. S. Mao, M. Martemianov, A. Martini, M. Matsyuk, W. Mei, L. Merola, R. Messi, S. Miscetti, A. Moalem, S. Moccia, M. Moulson, S. Müller, F. Murtas, M. Napolitano, A. Nedosekin, M. Panareo, L. Pacciani, P. Pagès, M. Palutan, L. Paoluzi, E. Pasqualucci, L. Passalacqua, M. Passaseo, A. Passeri, V. Patera, E. Petrolo, G. Petrucci, D. Picca, G. Pirozzi, C. Pistillo, M. Pollack, L. Pontecorvo, M. Primavera, F. Ruggieri, P. Santangelo, E. Santovetti, G. Saracino, R. D. Schamberger, C. Schwick, B. Sciascia, A. Sciubba, F. Scuri, I. Sfiligoi, J. Shan, P. Silano, T. Spadaro, S. Spagnolo, E. Spiriti, C. Stanescu, G. L. Tong, L. Tortora, E. Valente, P. Valente, B. Valeriani, G. Venanzoni, S. Veneziano, A. Ventura, Y. Wu, Y. G. Xie, P. P. Zhao, Y. Zhou

[2] *E-mail address: achim.denig@lnf.infn.it*

Table 1 $\phi(1020)$ Decays

ϕ decay	BR [%]	Events/year
K^+K^-	49.5	$9.8 \cdot 10^{10}$
$K^0\bar{K}^0$	34.4	$6.9 \cdot 10^{10}$
$\rho\pi$,$\pi^+\pi^-\pi^0$	15.5	$3.0 \cdot 10^{10}$
$\eta\gamma$	1.3	$2.6 \cdot 10^8$
$f_0\gamma$,$a_0\gamma$, $\eta'\gamma$	$\approx 10^{-2}...10^{-4}$	$\approx 2 \cdot 10^6...2 \cdot 10^8$

violation. The collinear production of the monochromatic [3] K_SK_L pair allows one to tag one of the kaons (with defined direction and identity) when the partner kaon had been identified.

In table 1 the main ϕ decays are summarized, together with the event yield at design luminosity in one "technical" year ($10^7 s$) of data taking. One notes that DAΦNE is not only a "factory" for kaon pairs but produces also at huge statistics ρ's, η's and the rare ϕ decays into $\eta'(958)$, $f_0(980)$ and $a_0(980)$. The physics program of KLOE is therefore complementary and goes beyond the study of symmetry violations (CP, CPT test)[2]. It covers - among many other studies - the analysis of kaon form factors, the investigation of rare ϕ decays, as well as the measurement of the hadronic cross section below the ϕ mass.

1.1 Measurement of ϵ'/ϵ

The KLOE detector is designed primarily with the goal of measuring the direct CP violation in K^0 decays with a sensitivity of $\approx 10^{-4}$ in $\Re(\epsilon'/\epsilon)$ [4] . The measurement of ϵ' has a long history, yielding in a first round of experiments (*NA31*, CERN and *E731*, FNAL) with contradictory results which only recently have been converging better (*NA48*, CERN [3] and *KTeV*, FNAL [4]). The world average of the two experiments $\Re(\epsilon'/\epsilon) = (2.1 \pm 0.5) \cdot 10^{-3}$ [5] indicates a value off 0 and therefore rules out the *superweak* postulate for the violation of the CP symmetry.

Double Ratio

KLOE will measure $\Re(\epsilon'/\epsilon)$ with a different experimental setup (collinear kaon pair production) than the CERN and FNAL experiments and hence with systematic errors from completely different sources. The double ratio R is the standard quantity measured to obtain $\Re(\epsilon'/\epsilon)$:

$$R = \frac{BR(K_L \to \pi^+\pi^-)/BR(K_S \to \pi^+\pi^-)}{BR(K_L \to \pi^0\pi^0)/BR(K_S \to \pi^0\pi^0)} = 1 + 6 \cdot \Re(\epsilon'/\epsilon). \tag{1}$$

[3] momenta: $\vec{p}_S = -\vec{p}_L$ with $|\vec{p}_{S,L}| = 110 MeV/c$; mean decay path: $\tau_S = 0.6$ cm, $\tau_L = 340$ cm

[4] A statistical error of $1 \cdot 10^{-4}$ can be achieved in ≈ 2 years of data taking at design luminosity.

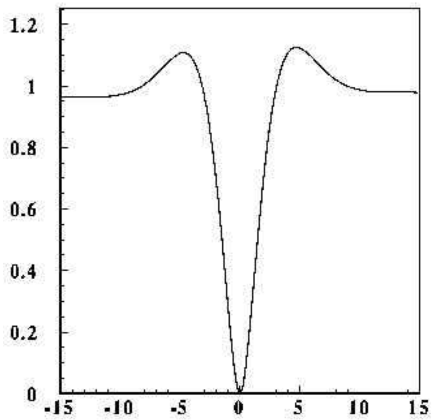

Fig. 1: Decay intensity (a.u.) as a function of $\Delta t/\tau_S$ for the neutral kaon pair decaying into $f_1 = \pi^+\pi^-$, $f_2 = \pi^0\pi^0$. The measurement of this interference patterns allows to extract ϵ'/ϵ.

The experimental goal is the measurement of the branching ratios $BR_{L,S;+-,00}$ of K_S and K_L into the $\pi^+\pi^-$ and $\pi^0\pi^0$ final state:

$$BR_{L,S;+-,00} = \frac{N^{Obs}_{L,S;+-,00} - N^{Bkg}_{L,S;+-,00}}{N_{KK} \cdot \epsilon^{Tag}_{L,S} \cdot \epsilon^{Rec}_{L,S;+-,00} \cdot \int\int_{FV} I(\vec{x}) \cdot G(\vec{x} - \vec{x}')d\vec{x}d\vec{x}'}, \tag{2}$$

where the total number of kaon pairs N_{KK} and the tagging efficiency $\epsilon^{Tag}_{L,S}$ drop out in the double ratio, while the reconstruction efficiency $\epsilon^{Rec}_{L,S;+-,00}$ has to be known at the 10^{-4} level. The decay intensity $I(\vec{x})$ is convoluted with the detector resolution $G(\vec{x}-\vec{x}')$ and requires an alignment of the fiducial volume (FV) with a precision of few millimeters. An important issue is the separation of the CP violating decays $K_L \to 2\pi$ from the CP conserving K_L decays ($K_L \to 3\pi$ and $K_L \to \pi l \nu_l, l = e, \mu$). The required background rejection is of the order 10^4 to 10^5 (depending on the signal channel) and makes use of the high resolution drift chamber and the hermetic electromagnetic calorimeter of KLOE (see next chapter).

Kaon Interferometry

At DAΦNE a novel phenomenon can be studied for the first time: interference patterns which arise due to the existence of two amplitudes in the initial quantum state of the neutral kaon system being produced in the ϕ decay with charge parity $C = -1$:

$$|i\rangle = \frac{1}{\sqrt{2}}(|K_L, \vec{p}\rangle|K_S, -\vec{p}\rangle - |K_L, -\vec{p}\rangle|K_S, \vec{p}\rangle) \tag{3}$$

The decay intensity I for the decay of the two kaons into the final states f_1 and f_2 is expressed in the following as a function of the time difference $\Delta t = t_1 - t_2$, where t_1 and t_2 are the individual decay times. The amplitude ratios $\eta_i = \langle f_i|K_L\rangle/\langle f_i|K_S\rangle$ contain the relevant parameters which describe CP violation ($\Delta m = m_L - m_S$):

$$I(f_1, f_2; \Delta t) = |\langle f_1|K_S\rangle\langle f_2|K_S\rangle|^2 \cdot [|\eta_1|^2 e^{-\Gamma_L \cdot \Delta t} + |\eta_2|^2 e^{-\Gamma_S \cdot \Delta t} - 2|\eta_1||\eta_2| e^{-\Gamma \cdot \Delta t/2} \cdot cos(\Delta m \Delta t + \Delta\varphi)] \quad (4)$$

One can thus perform a whole spectrum of "kaon-interferometry" experiments [6] with KLOE by measuring the above decay intensity distributions for different final states f_1, f_2. In total, one can determine the full set of parameters describing the system [5]. As an example the decay pattern for $f_1 = \pi^+\pi^-$ and $f_2 = \pi^0\pi^0$ is displayed in figure 1. Small asymmetries in the counting rate for large Δt and for $\Delta t \leq 5\tau_S$ are a measure of $\Re(\epsilon'/\epsilon)$ and of $\Im(\epsilon'/\epsilon)$ respectively. A good experimental vertex resolution for the charged and neutral decays is required to perform such an analysis.

1.2 Hadronic Physics

One of the first physics results of KLOE were obtained from the analyses of the radiative decays of the ϕ into the *scalar mesons* $f_0(980)$ and $a_0(980)$ [7]. The nature of these narrow states is unclear. Several models have been proposed which try to explain the total width (≈ 50 MeV) and the small $\gamma\gamma$ coupling (≤ 0.6 keV for f_0, ≈ 0.2 keV for a_0) which is very different from the $q\bar{q}$ expectation. At present the alternative models range from a four quark state $q\bar{q}q\bar{q}$ hypothesis to a kaonic molecule $K\bar{K}$ or models with a large strangeness or even gluonic content (see also in these proceedings [8] and references in [7]). The several models are predicting different branching ratios for the decays $\phi \rightarrow f_0\gamma$, $\phi \rightarrow a_0\gamma$, between $\approx 10^{-4}$ down to $\approx 10^{-6}$. A precise measurement of these decays can hence give a definite answer on the structure of the states.

The reason for studying ϕ radiative decays into the *pseudoscalars* η and η' is twofold. While the measurement of the $BR(\phi \rightarrow \eta'\gamma)$ can help to probe a large strangeness content of the η', the measurement of the ratio $R_\phi = BR(\phi \rightarrow \eta'\gamma)/BR(\phi \rightarrow \eta\gamma)$ allows one to extract the $\eta - \eta'$ mixing angle ϑ_P [9] for which no precise data exist (see also in these proceedings [10]).

In this paper we also present the results of an analysis of the reaction $\phi \rightarrow \pi^+\pi^-\pi^0$, where this final state can be reached either from the direct decay of the ϕ or via the ρ decay ($\phi \rightarrow \rho^\pm\pi^\mp, \rho^0\pi^0$).

Finally we will present a project which aims to measure the hadronic cross section using Initial State Radiation (ISR) events $e^+e^- \rightarrow \gamma\gamma^* \rightarrow \gamma\ hadrons$. The "radiative return" allows us to get a measurement of the hadronic cross section in the Q^2 invariant mass range $2m_\pi^2 \leq Q^2 \leq 1GeV^2$, even when DAΦNE is operating at a fixed center of mass energy $\sqrt{s} = m_\phi$. The precise knowledge of the hadronic cross section - especially at low energies - is of great interest for an improvement of the theoretical error of the muon anomaly a_μ and for the fine structure constant α_{em} at the Z^0 pole. The hadronic contributions of these fundamental quantities cannot be calculated in the framework of perturbative QCD and are rather obtained through dispersion integrals using as input experimental cross section data [11].

[5] also under the assumption of CPT - non-invariance or under a violation of the $\Delta S = \Delta Q$ rule.

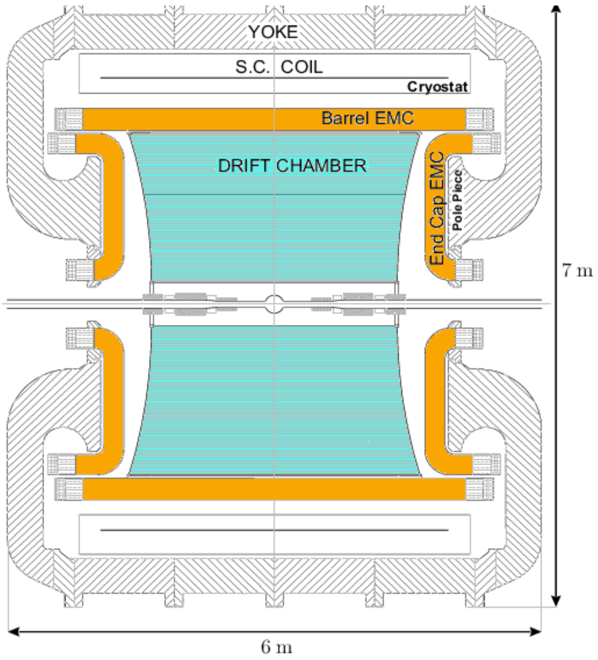

Fig. 2: Side view of the KLOE detector

2 The KLOE Detector

KLOE [12] [13] [14] (see figure 2.) is a typical e^+e^- general purpose detector with solenoid geometry, consisting of a very large helium based *drift chamber* (DC), surrounded by an *electromagnetic calorimeter* (EmC) and a superconducting magnet (0.6 T). The EmC consists of a barrel part and two endcap parts which are surrounding the cylindrical DC; a 98% hermetic coverage of the solid angle is achieved. The beam pipe around the interaction point (I.P.) has a spherical shape (10 cm radius, 500 μm thickness) which allows all K_S's to decay within this volume ($16K_S$ lifetimes). The DAΦNE beams are collimated close to the I.P. with a set of six permanent quadrupoles which are instrumented with two KLOE tile calorimeters (lead-scintillating tiles). This instrumentation helps to reject γ's which hit the quadrupoles. The detector acceptance is therefore increased, especially the discrimination of the CP violating decay $K_L \to \pi^+\pi^-$ from $K_L \to \pi^+\pi^-\pi^0$.

2.1 Electromagnetic Calorimeter

The EmC has been constructed for a precise detection of low energetic photons (down to ≈ 20 MeV). It has to discriminate $K_L \to 2\pi^0$ from $K_L \to 3\pi^0$ decays and to measure the $K_{S,L}$ neutral decay vertex with an accuracy of a few *mm*. Moreover the calorimeter

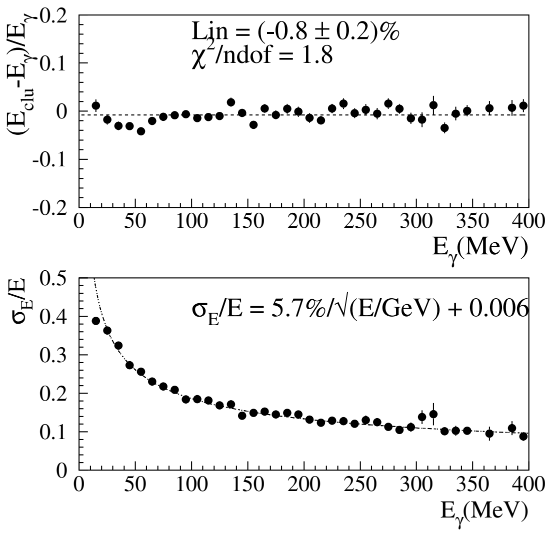

Fig. 3: Energy residuals and resolution of the EmC measured with radiative Bhabha events

serves as a fast, unbiased first level trigger. In order to fulfill these requirements, a detector has been constructed in which a matrix of scintillating fibres is embedded in lead. This construction results in an excellent timing and very good energy resolution (design values: $\sigma_E/E = 5\%/\sqrt{E(GeV)}$, $\sigma_t = 70ps/\sqrt{E(GeV)}$) with high detection efficiency.

The calorimeter energy calibration is performed using cosmic rays to equalize the cell response, plus Bhabha and $e^+e^- \to \gamma\gamma$ events to refine the equalization and to set the absolute energy scale. The linearity and the resolution as a function of energy are measured with radiative Bhabha events $e^+e^- \to e^+e^-\gamma$, where the photon energy is determined by the missing momentum (measured in the DC with the two charged tracks). The linearity is better than 1% over the full energy range $(20 - 400$ MeV); the energy resolution is found to be $\sigma_E/E = 5.7\%/\sqrt{E(GeV)}$ as can be seen in figure 3. The absolute energy calibration is checked by reconstructing the two-photon invariant mass for $\phi \to \pi^+\pi^-\pi^0$ events. We find a mass of $134.5 MeV/c^2$ ($\sigma = 14.7 MeV/c^2$) which is in good agreement with m_{π^0}.
After time equalization with cosmic rays, the time resolution as a function of energy is deduced from radiative Bhabha and ϕ radiative events: $\sigma_t = 54ps/\sqrt{E(GeV)} + 147$ns. Such a good timing performance translates to a neutral vertex resolution (measured with $K_L \to \pi^+\pi^-\pi^0$ events) of about 1.6 cm.

2.2 Cylindrical Drift Chamber

The KLOE drift chamber [15] has been designed to optimize the detection and reconstruction of the charged K_S and K_L decays, aiming at a precise determination of the decay vertex ($\approx 1mm$) and a very high momentum resolution of the low momenta tracks[6]. The mean decay path of the K_L is 340 cm; therefore the decay vertices are far from the I.P.. Thus, the chamber dimension, the drift cell shapes, the choice of magnetic field and gas mixture had to be optimized for these demanding requirements. The need for a very large fiducial volume led to a cylindrical drift chamber with 2 m radius and 3.3 m length. The isotropy of the decay products led us to a full stereo geometry of the drift cells which ensures the highest uniformity in filling the sensitive volume. Multiple scattering and photon conversion in the chamber walls are kept under control by employing low Z material (carbon fibre) in the chamber structure and the use of a low mass Helium based gas mixture (90% Helium, 10% Isobutane; $X_0 = 900$ m). The 12582 cells of the chamber are arranged in 58 circular layers. In order to improve the acceptance for the K_S decays, the inner 12 layers consist of 2x2cm^2 cells while the outer layers are made of 3x3cm^2 cells. Consecutive layers have stereo angles of opposite sign, with the stereo angles increasing with radius in order to achieve similar cell shapes all over the chamber (stereo angles from 60 mrad to 150 mrad).
Due to the peculiar cell geometry and the drift properties of the Helium based gas mixture, which is not saturated, the calibration of the space-to-time-relation of the DC is important and is done using cosmic ray events. The cell response gives a resolution of $\approx 150\mu$m over most of the drift distance. The momentum resolution for Bhabha events (see figure 4, left) is found to be better than the design value: $\sigma_{p_\perp}/p_\perp \leq 0.4\%$. The very good DC performance is illustrated also in figure 4 (right) where the invariant mass plot of $K_S \rightarrow \pi^+\pi^-$ is shown: $\sigma \approx 1MeV/c^2$.

2.3 Trigger and DAQ

The KLOE trigger [16] is designed to have a high (and almost equal) efficiency for the CP violating K_L decays and to downscale the rates from Bhabhas ($\approx$ 20 kHz), cosmic rays and machine background in order to keep the total DAQ rate below 10 kHz. The first stage (T1) of this 2-level-trigger provides a start to the FEE of the EmC, while the second stage (T2) serves as a validation trigger which stops the readout of the DC TDC's. T1 and T2 are based on the energy and topology of the deposits in the EmC and on the number of hits in the DC.
The DAQ system [17] handles 23000 FEE channels on an expected 2.5 kHz ϕ decay rate and $\approx$ 5 kHz properly downscaled background rate. The signal digitization occurs in 2 μs and the bandwidth is 50 MByte/s (at 5 kByte/event). The DAQ system has been fully tested at the design rates.

[6]The momenta of the K_L decays have a spectrum between $\approx 150MeV/c$ and 270 MeV/c

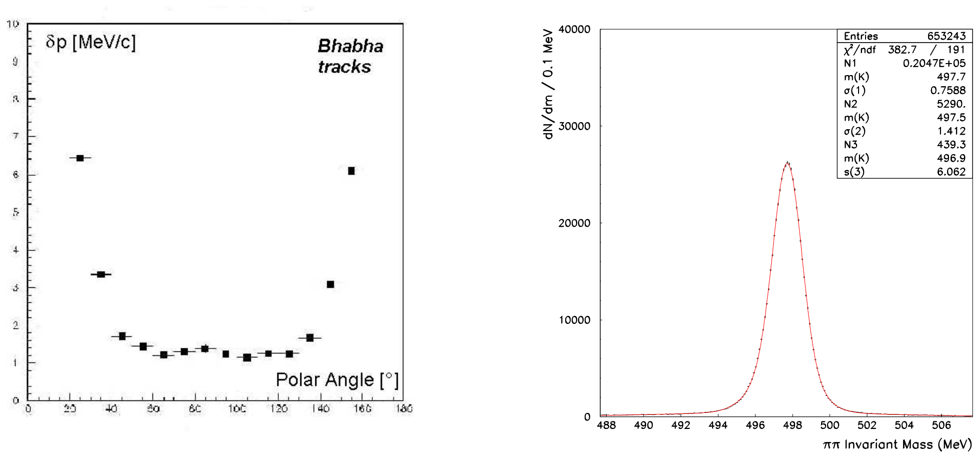

Fig. 4: KLOE drift chamber performance: In the left plot the momentum resolution for Bhabha events is drawn as a function of the polar angle of the tracks. The right plot shows the K_S invariant mass for $K_S \to \pi^+\pi^-$ and illustrates the excellent momentum resolution of the DC.

3 First Data Taking of KLOE

The first stable data taking of KLOE took place in December 1999. The collected integrated luminosity in 1999 is $\int \mathcal{L} dt = 2.4 pb^{-1}$, corresponding to about 8 million ϕ decays. After some hardware upgrades of the DAΦNE accelerator and a series of machine developments, the data taking started again in July 2000 with a peak luminosity $\geq 1 \cdot 10^{31} cm^{-2} s^{-1}$. The 1999 data has been used for the study and calibration of the detector performance (as discussed in the previous chapter), for the preliminary investigation of the systematics for the $\Re(\epsilon'/\epsilon)$ measurement (this chapter) and for the analysis of the radiative decays of the ϕ for which the results will be presented in more detail in the following chapter.

Tagging Strategies
The K_L can be tagged by a clearly identified $K_S \to \pi^+\pi^-$ event, for which the selection is a charged vertex with 2 tracks of opposite sign reconstructed close to the I.P. ($r \leq 6$cm, $|z| \leq 8$cm) and an invariant mass between 400 and $600 MeV/c^2$. The K_L tagging efficiency is found to be 72%; the background contamination is less than 1% (mainly $\phi \to K^+K^-$). An important check for the systematics of the K_S sample (and hence for the K_L tagging) is the measurement of the K_S lifetime which is possible by looking at the spatial difference between the secondary vertex $K_S \to \pi^+\pi^-$ and the e^+e^- primary vertex (luminous region). The measured K_S mean decay path is found to be in agreement with the expectation: $\lambda_S = (5.78 \pm 0.1)$ mm [18] [5].
A possibility to tag K_S's, is given by K_L particles which did not decay within the DC and are stopped in the EmC making a hadronic interaction ("K_L crash"). The excel-

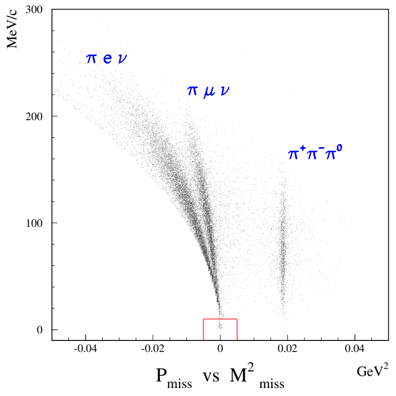

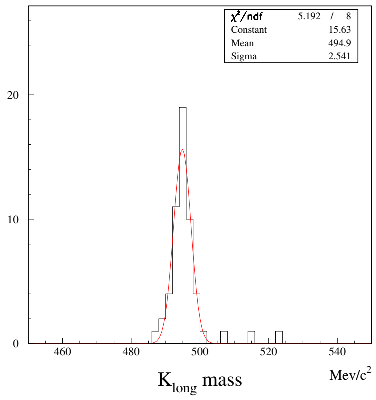

Fig. 5: The CP violating events $K_L \to \pi^+\pi^-$ can be selected in the two dimensional plane missing momentum vs. missing mass at $p_{miss} = 0, M^2_{miss} = 0$ (left plot). The mass distribution for the selected events (box, left) are shown in the right plot.

lent time resolution of the EmC is used to look for a neutral cluster within a velocity interval $0.195 \leq \beta \leq 0.245$ and with a cluster energy $E_{cluster} \geq 100$ MeV. The K_S tagging efficiency (percentage of identified K_S's via the K_L crash method) is 31%.

Fiducial Volume

An important issue for the measurement of the double ratio R is the control of the alignment of the K_L fiducial volume ($30cm \leq r \leq 150$cm, $|z| \leq 125$ cm). Since the vertex resolution for the $K_L \to \pi^+\pi^-$ and $K_L \to \pi^0\pi^0$ decay differs, a systematic error is introduced which is in the order of $\delta R = 4 \cdot 10^{-4}$ when the boundary of the fiducial volumes are shifted by $\delta r_{FV} = 5mm$. A control of the alignment is given by events with a reconstructable charged *and* neutral vertex, like e.g. $K_L \to \pi^+\pi^-\pi^0$. For those decays the residuals between the reconstructed charged ($\pi^+\pi^-$) and neutral ($\pi^0 \to \gamma\gamma$) vertices have been measured and were found to be below few millimeters.

Selection of $K_L \to \pi^+\pi^-$ events

The selection of the CP violating channel $K_L \to \pi^+\pi^-$ is based on the very good momentum resolution of the KLOE DC. In figure 5 (left) the two dimensional plane "missing momentum [7] vs. missing mass" is shown for charged K_L decays in which the K_L had been tagged before by $K_S \to \pi^+\pi^-$. The charged decay $K_L \to \pi^+\pi^-\pi^0$ and the semileptonic channels $K_L \to \pi\mu\nu_\mu$ and $K_L \to \pi e\nu_e$ are nicely separated from each other. Applying a loose cut ($p_{miss} \leq 10MeV/c$, $|M^2_{miss}| \leq (70MeV/c^2)^2$), the first CP violating events could be identified for which the mass distribution is shown in figure 5 (right).

[7] the missing momentum is evaluated in the pion mass hypothesis from the two charged tracks

4 Hadronic Physics at KLOE

In this chapter we will report on the first KLOE physics results which were obtained in the analysis of the radiative decays of the ϕ and the decay $\phi \to \pi^+\pi^-\pi^0$ (1999 data set [8]). The statistical errors for the BR measurements are already comparable to the precision obtained at the Novosibirsk VEPP-2M collider (see [7] and references there).

4.1 Radiative ϕ decays

4.1.1 $\phi \to f_0\gamma$ with $f_0 \to \pi^+\pi^-$

The signature for this decay are two charged tracks from the I.P. and a prompt photon. Two other processes lead to the same $\pi^+\pi^-\gamma$ final state: Initial State Radiation (ISR) in which the photon is emitted by the incoming e^- or e^+ and Final State Radiation (FSR) in which the γ is emitted by one of the pions. The latter process gives rise to an interference with the signal for which the sign of the interference term is still unknown. The selected $\pi^+\pi^-\gamma$ sample is hugely contaminated with radiative Bhabhas; a maximum likelihood method for an efficient $\pi - e$ separation has therefore been developed. For the identification of the signal $f_0 \to \pi^+\pi^-$, the Q^2 spectrum of the pion pair is used. In the region $Q^2 < 0.84GeV^2$ - where only ISR and FSR contribute to the final state - the experimental spectrum has been fitted with the theoretical event generator [22] and then extrapolated into the signal region ($Q^2 > 0.84GeV^2$). An excess of (35 ± 160) events is found which has been used to set an upper limit on the branching ratio: $BR(\phi \to f_0\gamma \to \pi^+\pi^-\gamma) < 1.64 \cdot 10^{-4}$ at 90% CL. In figure 6 the measured Q^2 spectrum is compared with the MC simulation (ISR and FSR only); both of them are in good agreement over the whole Q^2 range.

4.1.2 $\phi \to f_0\gamma$ with $f_0 \to \pi^0\pi^0$

The signature for the neutral decay of the $f_0(980)$ are 5 prompt photons in the EmC and no charged particle tracks in the DC. The main background comes from the non-resonant reaction $e^+e^- \to \omega\pi^0$ ($S/B = 0.5$); other background processes are $\phi \to \rho\pi^0$ and $\phi \to a_0\gamma \to \eta\pi^0\gamma$ with only photons in the final state. A two-step kinematic fit (with and without mass constraints) and suitable topological cuts are applied to reduce the background. The final detection efficiency is $\approx 40\%$. In a data sample of $1.8pb^{-1}$ (307 ± 18) $\pi^0\pi^0\gamma$ events have been selected; the expected background rate (estimated from Monte Carlo) is (112 ± 11). We find the following branching ratio for the neutral decay of the f_0: $BR(\phi \to f_0\gamma \to \pi^0\pi^0\gamma) = (0.80 \pm 0.09_{stat} \pm 0.06_{syst}) \cdot 10^{-4}$.
The same data sample has been used to select $\omega\pi^0$ events. Therefore different topological cuts have been applied resulting in (529 ± 23) accepted events at a background contamination of (93 ± 10) (estimated by Monte Carlo); we find the cross section at the ϕ mass for this process as: $\sigma_{e^+e^- \to \omega\pi} = (0.67 \pm 0.04_{stat} \pm 0.05_{syst})nb$.

[8] The results are preliminary. A complete analysis of the systematic effects as well as the analysis of the year 2000 data is going on. At present (Oct. 2000) the collected integrated luminosity *per week* is considerably higher than the full 1999 data set for which results are presented here.

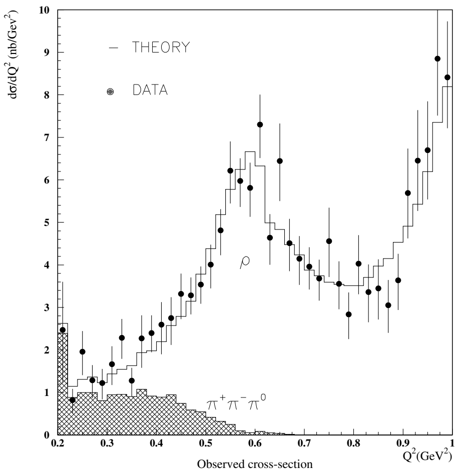

Fig. 6: Experimental cross section as a function of Q^2 for $\pi^+\pi^-\gamma$ events ($45^o \leq \Theta \leq 135^o$ for Θ_π, Θ_γ). The data is compared with the MC simulation under the assumption of pure ISR and FSR. At the given statistical resolution no signal $f_0 \rightarrow \pi^+\pi^-$ can be seen.

4.1.3 $\phi \rightarrow a_0\gamma$ with $a_0 \rightarrow \eta\pi^0 \rightarrow 4\gamma$ $(\eta \rightarrow \gamma\gamma)$

Events are selected with a signature of 5 prompt photons and the abscence of a charged track in the detector. The main background process is the decay discussed in the previous subchapter $\phi \rightarrow f_0\gamma \rightarrow 5\gamma$ $(S/B = 0.1)$ and $\phi \rightarrow \eta\gamma$ $(\eta \rightarrow \pi^0\pi^0)$. A constrained kinematic fit and topological cuts are applied to reduce this background. There have been (74 ± 9) $\eta\pi^0\gamma$ events selected (23% detection efficiency) with a background of (21 ± 6) events (MC estimate), corresponding to a branching ratio $BR(\phi \rightarrow a_0\gamma \rightarrow \omega\pi^0\gamma) = (0.77 \pm 0.15_{stat} \pm 0.10_{syst}) \cdot 10^{-4}$.

4.1.4 $\phi \rightarrow \eta\gamma$, $\phi \rightarrow \eta'\gamma$

We are studying four processes, giving rise to two different final states: $\phi \rightarrow \eta(\eta')\gamma \rightarrow \pi^+\pi^-\pi^0(\pi^+\pi^-\eta)\gamma \rightarrow \pi^+\pi^-3\gamma$ and $\phi \rightarrow \eta(\eta')\gamma \rightarrow \pi^0\pi^0\pi^0(\pi^0\pi^0\eta)\gamma \rightarrow 7\gamma$. We use both decay chains to construct separately the ratio $R_\phi = BR(\phi \rightarrow \eta'\gamma)/BR(\phi \rightarrow \eta\gamma)$ in which most of the selection efficiencies (e.g. trigger efficiency) and all the normalisation efficiencies (luminosity, ϕ cross section) cancel.
The $\phi \rightarrow \eta\gamma$ is the main background for the rare corresponding $\phi \rightarrow \eta'\gamma$ decay (see Table 1), but - since the η decay can be selected almost background free on a simple topological basis - they constitute also an important control channel for testing the systematics. Comparison between data and Monte Carlo (see figure 7) show a very good agreement for the η channel.

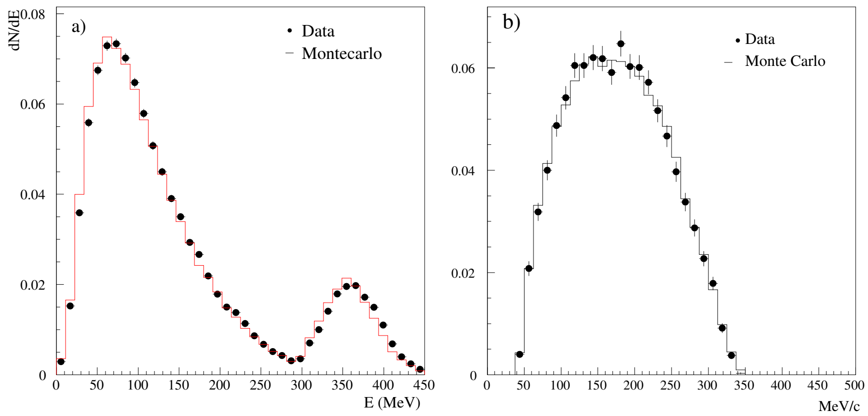

Fig. 7: Comparison Data - Monte Carlo for the $\phi \to \eta\gamma$ sample: photon energy spectrum in 7γ events (left plot); charged pions momentum spectrum in $\pi^+\pi^-3\gamma$ events (right).

The event selection is based on a first level kinematic fit with mass constraints, followed by a selection which uses the χ^2 probability for the hypotheses of an event to be either $\eta\gamma$ or $\eta'\gamma$ like. After this procedure we are left with (21 ± 4.6) η' events in the $\pi^+\pi^-3\gamma$ final state and with $6^{+3.3}_{-2.2}$ in the 7γ final state with less than one expected background event at 90% CL. This is the first observation of the $\phi \to \eta'\gamma \to 7\gamma$ decay chain. Using the number of selected η and η' events, the efficiencies evaluated by Monte Carlo and the intermediate states BR's as given by PDG [5] we evaluate the ratio $R_\phi = (7.1 \pm 1.6_{stat} \pm 0.3_{syst}) \cdot 10^{-3}$ or BR($\phi \to \eta'\gamma$)=$(8.9 \pm 2_{stat} \pm 0.6_{syst}) \cdot 10^{-5}$. This result has the same level of accuracy as the current world average. Using a formula proposed by Bramon [19] we can use this value of R_ϕ to extract the $\eta - \eta'$ mixing angle: $\vartheta_P \simeq -19°$. The value of the BR($\phi \to \eta'\gamma$) disfavours models with large gluonium admixtures of the η'.

4.2 $\phi \to \pi^+\pi^-\pi^0$

$\pi^+\pi^-\pi^0$ events are selected requiring a prompt vertex with two opposite sign tracks in the DC and two prompt photons in the EmC. Cuts on the opening angle of the tracks and on the two photons are applied for background subtraction. The data has been analyzed by means of Dalitz plots. The Dalitz plot (binned in 8×8 MeV squares and corrected for the efficiency) is fitted to a model of $\pi^+\pi^-\pi^0$ production including the following terms:

- $A_{\rho\pi}$ is the $\rho\pi$ amplitude given by the sum of the three ρ states, each described by a Gounaris-Sakurai parametrization. Free parameters are the ρ masses and the width;
- A_{direct} is the direct term contribution given by a complex number. The modulus is normalized in such a way that a value equal to 1 corresponds to a direct term equal to the $\rho\pi$ term.

Parameter	Fit result	PDG result
$M(\rho_0)$ (MeV)	776.1 ± 1.0	776.0 ± 0.9
ΔM (MeV)	-0.5 ± 0.7	0.1 ± 0.9
$\Gamma(\rho)$ (MeV)	145.6 ± 2.2	150.9 ± 2.0
A(direct term)/A($\rho\pi$)	0.10 ± 0.01	$-0.15 \div 0.11$
phase(direct term)-phase($\rho\pi$)	$(114 \pm 12)^o$	

Table 2 Results of the fit to the $\pi^+\pi^-\pi^0$ Dalitz plot compared with the PDG values.

- $A_{\omega\pi}$ is the $\omega\pi$ term, where mass and width of the ω are fixed to the PDG values, and only a complex amplitude (modulus and phase) is left free.

The fitting function is then given by: $f(X,Y) = |\vec{p}^{\,+} \times \vec{p}^{\,-}|^2 \cdot |\mathbf{A}_{\rho\pi} + \mathbf{A}_{\mathbf{direct}} + \mathbf{A}_{\omega\pi}|^2$ (X and Y are two Dalitz variables). In Table 2 the results of the fit are shown and compared with PDG values.
First, we observe a sizeable direct term (about 10 % of the $\rho\pi$ amplitude) with a phase respect to $\rho\pi$ not too far from 90^o. We remark that this is the first observation of this decay. Second we find values of the ρ line-shape parameters which are in agreement with PDG [5] numbers. Furthermore the mass difference between the neutral and the charged ρ's is compatible with 0; hence no isospin violation is observed.

4.3 Measurement of the hadronic cross section

At KLOE we plan to perform a high precision measurement of the hadronic cross section below the ϕ mass *using ISR events*: $e^+e^- \to \gamma\gamma^* \to \gamma$ *hadrons* [20] [21]. This measurement can significantly reduce the theoretical error of a_μ and $\alpha_{em}(m_Z^2)$ (see motivation in chapter 1). We are concentrating on the measurement of the hadronic cross section for the reaction $e^+e^- \to \rho\gamma \to \pi^+\pi^-\gamma$ as a function of Q^2 ($\pi\pi$ invariant mass) which allows us to extract the cross section of the dominating hadronic process at low energies: $\sigma(e^+e^- \to \pi^+\pi^-)$ [9]. We would like to stress that the method to use ISR events (while DAΦNE is operating at a fixed beam energy) is a complementary approach to the conventional energy scan. In the case of the ISR method, many systematic effects (e.g. luminosity, beam energy measurement) enter only *once*, while they have to be determined for *each* energy step in the case of a variable beam energy.
An important issue for this measurement is the suppression of FSR. Monte Carlo simulations [22] showed that a restriction of the photon polar angle ($10^o \leq \Theta_\gamma \leq 40^o$) and energy ($E_\gamma \geq 50MeV$) suppresses FSR below 1%.
From a data sample of $1.8pb^{-1}$ we selected $\pi^+\pi^-\gamma$ events like described in section 4.1.1 (search for $f_0 \to \pi^+\pi^-$) and we reduced the huge radiative Bhabha contamination (maximum likelihood method). We find a good agreement of the experimental Q^2 distribution with the Monte Carlo simulation, profing that the experimental techniques

[9] The $\pi^+\pi^-\gamma$ cross section is enhanced due to the coupling of the virtual photon to the ρ in the case of ISR: $e^+e^- \to \gamma^*\gamma \to \rho\gamma \to \pi^+\pi^-\gamma$

(detector performance, selection criteria) and the theoretical description are good. The final goal to reduce δa_μ^{hadr} to $\approx 1.5 \cdot 10^{-10}$ in the energy range below the ϕ resonance (the main contribution coming from the $\pi^+\pi^-$ cross section) requires an integrated luminosity of $\approx 100pb^{-1}$.

5 Conclusions

The KLOE detector has started its operation in 1999 and has shown to be fully operational in all its hardware and software components, reaching or being very close to its design specifications. Using the $2.4pb^{-1}$ delivered luminosity in 1999, the first physics results in the analysis of the radiative decays of the ϕ were obtained which have a precision comparable or even better than the world data sample. Those results will improve substantially with the data taken in 2000. A series of new measurements - also in the field of kaon decays - are in preparation and the systematics for the measurement of CP violation can be further studied with the new data. The next milestone is a measurement of $\Re(\epsilon'/\epsilon)$ with a precision of $\approx 10^{-3}$ which requires an integrated luminsity of $100pb^{-1}$ to be provided by DAΦNE. The KLOE detector is ready for this goal.

6 Acknowledgement

The author would like to thank the organizers for the possibility to present the KLOE experiment and its results at *Hadron Structure 2000.* The conference offered us a rich and varied physics program in the pleasant High Tatras Mountains.

References

[1] C.Milardi: *Proc. DAΦNE'99* **Frascati Physics Series XVI** (1999) 75;

[2] J.Lee-Franzini: **The Second DAΦNE Physics Handbook** (1995) 761;

[3] The NA48 Collaboration: *Phys. Lett.* **B 465** (1999) 335;

[4] The KTeV Collaboration: *Phys. Rev. Lett.* **83** (1998) 22;

[5] The Particle Data Group: *Europ. Phys. Jour.* **C 15** (2000) 1;

[6] C.D.Buchanan et al.: *Phys. Rev.* **D 45** (1992) 4088;

[7] The KLOE collaboration: *KLOE first Results on Hadronic Physics: Proc. XXXth Int. Conf. on High Energy Physics, Osaka, Japan* (2000) ;

[8] R. Escribano: *these proceedings* (2000) ;

[9] J.L.Rosner: *Phys. Rev.* **D 27** (1983) 1101;

[10] A. Bramon: *these proceedings* (2000) ;

[11] S.Eidelman, F.Jegerlehner: *Z.f.Physik* **C 67** (1995) 585;

[12] The KLOE collaboration: *A Gen. Purp. Detect. for DAΦNE* **LNF-92/019** (1992) ;

[13] The KLOE collaboration: *The KLOE Detet.; Techn. Prop.* **LNF-93/002** (1993) ;

[14] The KLOE collaboration: *Novel DAQ and Trigger Methods for the KLOE Experiment: Proc. XXXth Int. Conf. on High Energy Physics, Osaka, Japan* (2000) ;

[15] The KLOE collaboration: *The KLOE Drift Chamber* **LNF-94/028** (1993) ;

[16] The KLOE collaboration: *The KLOE Trigger System* **LNF-96/043** (1996) ;

[17] The KLOE collaboration: *The KLOE Data Acquisition System* **LNF-95/014** (1995) ;

[18] The KLOE collaboration: *First Results from $\phi \to K_L K_S$ Decays with the KLOE Detector: Proc. XXXth Int. Conf. on High Energy Physics, Osaka, Japan* (2000) ;

[19] A.Bramon: *Europ. Phys. Jour.* **C 7** (1999) 271;

[20] S.Spagnolo: *Europ. Phys. Jour.* **C 6** (1999) 637;

[21] A.Denig: *Proc. DAΦNE'99* **Frascati Physics Series XVI** (1999) 569;

[22] S.Binner et al.: *Phys. Lett.* **B 459** (1999) 279;